IIETA International Information and Engineering Technology Association
Advancing the World of Information and Engineering

Mathematical Modelling of Engineering Problems
Vol. 9, No. 4, August, 2022, pp. 1123-1130
Journal homepage: http://iieta.org/journals/mmep

Design of Integral Sliding Mode Control for Seismic Effect Regulation on Buildings with Unmatched Disturbance

Suha S. Husain*, Taghreed MohammadRidha

Control and Systems Eng. Dept., University of Technology - Iraq, Baghdad 10066, Iraq

Corresponding Author Email: 11698@uotechnology.edu.iq

https://doi.org/10.18280/mmep.090431

Received: 9 June 2022
Accepted: 23 August 2022

Keywords:
sliding mode control, integral sliding mode control, unmatched disturbance, magnetorheological damper, MRD, seismic effect, regulation buildings, earthquakes, structural building

ABSTRACT

In this work the robustness properties of Integral Sliding Mode Controller (ISMC) are studied for the problem structural vibration. Selecting the sliding manifold which takes into account the attenuation of the unmatched perturbation is studied as well. This study has two scenarios the first is comparing two types of sliding mode controllers which designed to control 3-story scaled structure supported by Magneto Rheological Damper (MRD). ISMC is compared to classical Sliding Mode Control (SMC) performance, the two controllers checked under effect of Mexico city earthquake. The second scenario compares the proposed controller with other controllers from literature under effect of time scaled El Centro 1940 earthquake. The results show that ISMC performance is better than SMC in scenario one and better than other controllers in scenario two. All the simulation results are obtained by MATLAB.

1. INTRODUCTION

In the long run, buildings have suffered significant damage due to earthquakes. There are a lot of statistics on human and material damage caused by earthquakes, on average, about 10,000 people lose their lives due to earthquakes each year [1]. So many researchers in this field have sought to reduce the vibrations of structures to ensure the safety of humans and structures. Several techniques have emerged to reduce vibrations of structures, one of these techniques is passive control, which dissipates energy caused from seismic effect [2], this type of control vibration does not have feedback signal, therefore it is not sufficient [3]. New type of controller is active control, Active control dissipates energy and have feedback signal to correct the structure displacement [4]. Active devices have been used in many studies [5-9]. Active control needs a high power source [10-12], so this challenge led to a semi-active control which does not need a high power source because it works on the battery power [13-15].

Several control techniques have been applied with the semi-active device such as MRD, where MRD contains a liquid that quickly changes from liquid to semi solid in parts of seconds whether a magnetic field or an electric field is applied to it [16]. The control techniques are applied with MRD are divided into three sections, classic control, intelligent control and robust control. Jagadisha et al. [17] designed Proportional Integral Derivative controller (PID) to drive MRD to control three-story scaled structure. Zizouni et al. [18] proposed Linear Quadratic Regulator (LQR) with MRD to reduce the seismic effect for three-story scaled structure.

In terms of intelligent control, Zizouni et al. [19] designed neural network controller to minimize earthquake effect on a scaled structure with MRD. The design is tested under two types of simulated earthquakes, Tōhoku earthquake and Boumerdès earthquake. The maximum redaction for the top floor displacement under the two types effect is 67.14% and 57.64% respectively as compared to the uncontrolled displacement.

Finally, we mention some of the studies that designed robust control to reduce the seismic effect on structures. Humaidi et al. [20] and Fali et al. [21] proposed Adaptive Sliding Mode Controller (ASMC) with MRD to control scaled structure, they compared ASMC performance with SMC, from the obtained results they concluded that ASMC is better than SMC in reducing the structure displacement.

From the observation of previous studies SMC has proven its effectiveness in overcoming the seismic effect but there are some points that have not been studied before that are covered here. Firstly, ISMC is designed for the first time for reducing structural vibrations. This controller does not have reaching phase that is found in classical SMC [22-25]. Secondly, the unmatched disturbance is taken into consideration for the first time in the design for this system.

In this study ISMC is designed to control MRD for the first time to reduce seismic structural vibrations. ISMC is compared with other controllers from literature to show its efficiency [26, 27].

This paper is organized as follows: the mathematical model of a building with MRD is presented in section 2. Integral sliding mode control design is explained in section 3. In section 4, the results are presented and discussed. Finally, the conclusion is presented in section 5

2. MATHEMATICAL MODEL OF THE BUILDING WITH AN MRD

The mathematical model of a building is shown in Eq. (1) [21, 27]:

$$\boldsymbol{M}\ddot{\boldsymbol{x}}(t) + \boldsymbol{C}\dot{\boldsymbol{x}}(t) + \boldsymbol{K}\boldsymbol{x}(t) = \boldsymbol{M}\boldsymbol{\Lambda}\ddot{x}_g(t) - \boldsymbol{\Gamma}\, F_c(t) \quad (1)$$

where, $\boldsymbol{x}, \dot{\boldsymbol{x}}\ and\ \ddot{\boldsymbol{x}}$ are displacement, velocity and acceleration vectors of the structure respectively. $\boldsymbol{x} = [x_1, x_2, x_3, \dots., x_n]^T$, n is the number of floors and in this work $n = 3$. $\boldsymbol{C}, \boldsymbol{K}$ and $\boldsymbol{M} \in R^{n*n}$ are damping, stiffness and mass matrices. $\ddot{x}_g$ is the unknown earthquake acceleration. $\boldsymbol{\Lambda} \in R^{n*1}$ is unity vector, F_c is the force produced by the dampers, $\boldsymbol{\Gamma} \in R^{n*1}$ represent the location of each damper. In this work one damper will be considered, hence:

$$\boldsymbol{\Gamma} = [0, 0, 0, 0, 0, 1]^T \quad (2)$$

State space representation for (1) is as follows:

$$\dot{\boldsymbol{x}} = \boldsymbol{A}\boldsymbol{x} + \boldsymbol{B}u + \boldsymbol{D}\,\ddot{x}_g \quad (3)$$

where, $\boldsymbol{B}\ and\ \boldsymbol{D}$ are $\in R^{2n*1}$, $\boldsymbol{A} \in R^{2n*2n}$, $u = F_c$. These matrices are as flows:

$$\boldsymbol{A} = \begin{bmatrix} \boldsymbol{0} & \boldsymbol{I} \\ -\boldsymbol{M^{-1}K} & -\boldsymbol{M^{-1}C} \end{bmatrix}, \boldsymbol{B} = \begin{bmatrix} \boldsymbol{0} \\ -\boldsymbol{M^{-1}\Gamma} \end{bmatrix}, \boldsymbol{D} = -\begin{bmatrix} \boldsymbol{0} \\ \boldsymbol{\Lambda} \end{bmatrix}.$$

For the system in Eq. (3) the vector D contains two parts the first on is D_1 which is represent the vector of match disturbance, while the second part represented by D_2 which is the vector of unmatched disturbance as the following:

$$D = D_1 + D_2$$

Rewrite the system formulation as follows:

$$\dot{\boldsymbol{x}} = \boldsymbol{A}\boldsymbol{x} + \boldsymbol{B}u + \boldsymbol{B}\,D_0\,\ddot{x}_g + f_u \quad (4)$$

where, $D_1 = \boldsymbol{B}D_0$ and $f_u = D_2\,\ddot{x}_g$.

$$f_u = D_2\,\ddot{x}_g \quad (5)$$

The nonlinear model of MRD which described by the modified Bouc–Wen model, this model was proposed by Zizouni et al. [18, 26]. The applied force suggested by this model is governed by the following equations:

$$F_c = c_1\dot{y} + k_0\,(x - y) + k_1(x - x_o) + \alpha z \quad (6)$$

$$\dot{y} = \frac{1}{c_0 + c_1}(c_o\dot{x} + k_o(x - y) + \alpha z) \quad (7)$$

$$\dot{z} = -\Upsilon|\dot{x} - \dot{y}|z|z|^{r-1} - \beta(\dot{x} - \dot{y})|z|^r + a(\dot{x} - \dot{y}) \quad (8)$$

where, x and $\dot{x}$, are displacement and velocity of the damper respectively, F_c, z, k_o and k_1 are generated force, hysteretic component, accumulator stiffness respectively at low and high velocity. Υ, β, r and a are parameters giving the shape and scale of the hysteresis loop. c_o and c_1 are the viscous damping at low and high velocity respectively, which depend on control voltage as see in Eqns. (9), (10) (11) and (12) respectively:

$$\alpha = \alpha_a + \alpha_b\mu \quad (9)$$

$$c_1 = c_{1a} + c_{1b}\mu \quad (10)$$

$$c_o = c_{oa} + c_{ob}\mu \quad (11)$$

$$\dot{\mu} = -\eta(\mu - v_c) \quad (12)$$

where, η is time response factor, μ is a phenomenological variable enveloping the system and v_c is the command voltage applied to the control circuit of the damper.

The resulting supplied control voltage of MRD is as follows [18, 26, 27]:

$$v_c = v_{max}H[(f_s - F_c).F_c] \quad (13)$$

where, v_{max} is maximum applied voltage, f_s the output force of controller (control force) and F_c force generated by MRD. $H(.)$ is a Heaviside step function.

3. CONTROL DESIGN

SMC is a robust control, which reject matched perturbation, So it is widely used due to its preferred robust performance [28-31]. SMC has two phases, reaching phase and sliding phase. During reaching phase the system is affected by the perturbation, while during sliding phase the system is not affected by it [15, 25]. Therefore, it is desired to reduce or even remove the reaching phase. ISMC eliminates the reaching phase in it is design [32], in addition ISMC can attenuate the unmatched disturbance by suitable selection of sliding manifold [23, 33].

For the system in Eq. (4) with $\boldsymbol{A} \in R^{6*6}$, and $\boldsymbol{D}, \boldsymbol{B}, \boldsymbol{D_1}, \boldsymbol{D_2}, \boldsymbol{M} \in R^{6*1}$.

Assume the upper bound of matched and unmatched disturbance is known.

Classical SMC and ISMC are designed next to compare their performances.

3.1 Classical SMC design

In this sub section design of SMC for the system in Eq. (4) will be discussed. Firstly the design of sliding surface is defined as follows:

$$\sigma = G\,\boldsymbol{x} \quad (14)$$

where, G vector is designed as $G = [g_1\ g_2\ g_3\ g_4\ g_5\ g_6]$, and $G\boldsymbol{B}$ is nonsingular square matrix. In order to analyze the sliding motion associated with the sliding manifold, The derivative of sliding manifold is given in Eq. (15):

$$\dot{\sigma} = G\,\dot{\boldsymbol{x}} = G\big(A\,\boldsymbol{x} + \boldsymbol{B}\,u + \boldsymbol{B}D_0\,\ddot{x}_g + f_u\big) \quad (15)$$

To ensure the sliding manifold attractiveness the following condition must be satisfied [23, 34];

$$\dot{\sigma} = G\,\dot{\boldsymbol{x}} = G\big(A\,\boldsymbol{x} + \boldsymbol{B}\,u + \boldsymbol{B}D_0\,\ddot{x}_g + f_u\big) \quad (16)$$

Select control low as

$$u = (GB)^{-1}(u_n + u_d) \quad (17)$$

where, $u_n\ and\ u_d$ are the nominal controller and discontinuous controller respectively which are designed as follows;

$$u_n = -GA\boldsymbol{x}, u_d = -K_0\,sign(\sigma) \quad (18)$$

K_0 is positive switching gain, will be designed next, after substuating Eq. (18) in Eq. (17) than in Eq. (15), the result is Eq. (19);

$$\sigma\,\dot{\sigma} \;\le\; -\|\sigma\|\left[K_0 \;- G\boldsymbol{B}D_0\ddot{x}_g - Gf_u\right] \tag{19}$$

Switching gain must satisfy the following condition in order to ensure the sliding manifold attractiveness:

$$K_0 \;> G\boldsymbol{B}D_0\ddot{x}_g + Gf_u + \eta \tag{20}$$

where, η is very small positive constant. During sliding $u = u_{eq}$ as the follows:

$$u_{eq} = (GB)^{-1}[-GA\boldsymbol{x} - GBD_0\ddot{x}_g - Gf_u] \tag{21}$$

The system dynamics during sliding is obtained by substituting Eq. (21) in Eq. (4) the result is as follows:

$$\begin{aligned}\dot{\boldsymbol{x}} = [I - B(GB)^{-1}G]A\boldsymbol{x} + [I - B(GB)^{-1}G]\,BD_0\ddot{x}_g \\ + [I - B(GB)^{-1}G]\,f_u\end{aligned} \tag{22}$$

Define $\Gamma = [I - B(GB)^{-1}G]$, then Eq. (22) will become:

$$\dot{\boldsymbol{x}} = \Gamma A\boldsymbol{x} + \Gamma\,BD_0\ddot{x}_g + \Gamma\,f_u \tag{23}$$

Note that when the sliding manifold is reached $\Gamma B = 0$ for $t \ge t_s$, (where t_s is represent reaching time to the sliding manifoled) then Eq. (23) becomes:

$$\dot{\boldsymbol{x}} = \Gamma A\boldsymbol{x} + \Gamma\,f_u \tag{24}$$

From the above analysis note that the matched disturbance is completely rejected while the unmutched disturbance depends on selection of sliding manifold.

3.2 ISMC design

To design ISMC, the sliding manifold is designed first as follows: The basic idea of ISMC design is to enforce a sliding mode from the first instant, as well as therefore ISMC eliminate reaching phase [22]. The first step in the design procedure is to design the sliding surface:

$$\sigma = G\,\boldsymbol{x} + Z \tag{25}$$

where, σ is the sliding manifold, Z is the integral term, $G \in R^{1*6}$ is to be designed. The derivative of sliding manifold and the integral term which will be used to prove attractiveness of sliding manifold is:

$$\dot{\sigma} = G\dot{x} + \dot{Z} \tag{26}$$

$$\dot{Z} = \; -GA\,x - (GB)u_n \tag{27}$$

Finally, ISMC control action produced in Eq. (28);

$$u = u_n + u_d \tag{28}$$

where, u_n and u_d defined as

$$u_n = B^{-1}[-\boldsymbol{A}\boldsymbol{x} - K\boldsymbol{x}], u_d = \; -K_0\,sign(\sigma) \tag{29}$$

where, K is gain vector which can calculated by Ackermann's formula. The choice of nominal controller (u_n) depend on some desired performance during sliding.

To ensure attractiveness of sliding surface σ the condition Eq. (19) must be satisfied [23, 34];

$$\sigma\,\dot{\sigma} \;\le\; -\|\sigma\|\left[K_0 \;- D_0\ddot{x}_g - Gf_u\right] \tag{30}$$

Switching gain must satisfy the following condition in order to ensure the sliding manifold attractiveness:

$$K_0 \;> D_0\ddot{x}_g + Gf_u + \eta \tag{31}$$

During sliding, the equivalent control of u_d is yielded:

$$[u_{eq}]_d = (GB)^{-1}[-GBD_0\ddot{x}_g - Gf_u] \tag{32}$$

Then the system dynamics during sliding is obtained by substituting Eq. (32) in Eq. (4):

$$\dot{\boldsymbol{x}} = (A - BK)\boldsymbol{x} + \Gamma\,f_u \tag{33}$$

For matched disturbance need only (GB)nonsigular, but for unmatched disturbance need specific selection of sliding surface. From Eq. (33) note that:

1- The effect of matched disturbance is completely rejected.
2- Γ can amplify the unmatched disturbance, therefore to avoid the amplification of the latter, use the following sliding manifold

$$G = (\boldsymbol{B^T B})^{-1}\boldsymbol{B^T} \tag{34}$$

This choice of G not only avoid amplification of unmatched disturbance but also has the simplifying property as follows [23]:

$$G\boldsymbol{B} = (\boldsymbol{B^T B})^{-1}\boldsymbol{B^T B} = \boldsymbol{I_m} \tag{35}$$

To ensures that the square matrix GB is nonsingular. With the choice of G in Eq. (34) the projection operator Γ becomes:

$$\Gamma = [I - B(B^T B)^{-1}B^T] \tag{36}$$

Note that Γ symmetric and idempotent, $\Gamma = \Gamma^2$. The properties of symmetry and idempotency imply that $\|\Gamma\| = 1$ which means that the effect of f_u is not amplified since $\|\Gamma f_u\| \;\le \|f_u\|$.

In fact the choice of G in Eq. (34) represent the optimal choice of sliding manifold [23, 33]. This choice of G is compared to a classical choice that is used in the literature.

4. RESULT AND DISCUSSION

In this section a three-story scaled structure is given as a case study with MRD as actuator whose parameters are given in Table 1 and Table 2 respectively. All the results are obtained by MATLAB/ SIMULINK. All the initial conditions are set to zero, which means that system starts from rest. The results are categorized into three scenarios. Firstly, ISMC performance is compared to SMC. In the second scenario ISMC with MRD is compared to other control algorithms from literature [26, 27].

To avoid chattering phenomena which caused by discontinuous part of controller (u_d) [35], the following approximation will be used:

$$sign(\sigma) \approx \frac{\sigma}{|\sigma| + \varepsilon} \tag{37}$$

where, ε is a very small positive constant. The three-story scaled structure parameter and MRD parameters are given in Table 1 and Table 2 respectively [26].

Table 1. System parameters

Parameter name	Parameter value
Mass matrix (M) Kg	$\begin{bmatrix} 98.3 & 0 & 0 \\ 0 & 98.8 & 0 \\ 0 & 0 & 98.3 \end{bmatrix}$
Damping matrix (C) $N.s/m$	$\begin{bmatrix} 175 & -50 & 0 \\ -50 & 100 & -50 \\ 0 & -50 & 50 \end{bmatrix}$
Stiffness matrix (K) N/m	$10^5 \times \begin{bmatrix} 12 & -6.84 & 0 \\ -6.84 & 13.7 & -6.84 \\ 0 & -6.84 & 6.84 \end{bmatrix}$

Table 2. MRD parameters

Parameter name	Parameter value
c_{0a}, c_{0b} $N.s/cm$	21 $N.s/cm$ 3.5
k_0, a	46.9 N/cm, 301
c_{1a}, c_{1b}	283 $N.s/cm$ 2.95 $N.s/cm$
r	2
α_a, α_b	$140\frac{N}{cm}$, $695\ N/cm$
Υ, β	363 cm^{-2}, 363 cm^{-2}
η, x_0	$190s^{-1}$, 14.3 cm
v_{max}	$2.25v$

First Scenario: The uncontrolled displacement of three-story scaled structure under effect of time scaled Mexico City earthquake which shown in Figure 1 are shown in Figure 2.

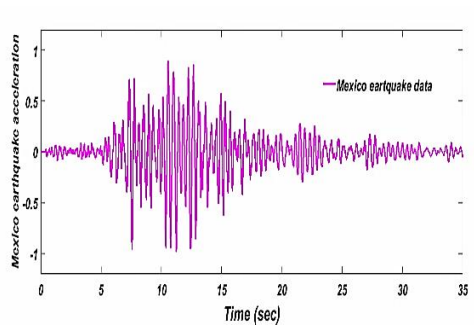

Figure 1. Time scaled Mexico City earthquake

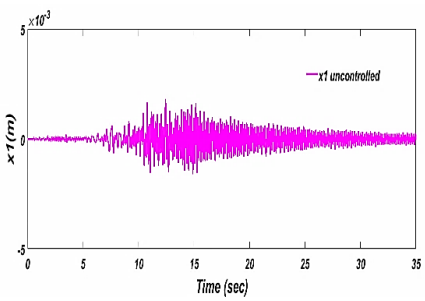

(a)

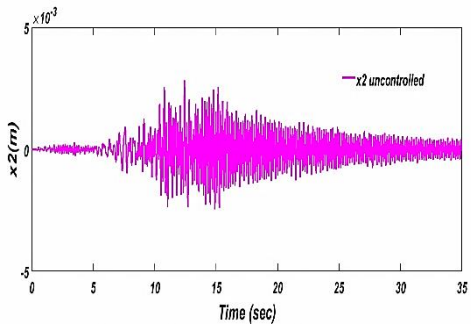

(b)

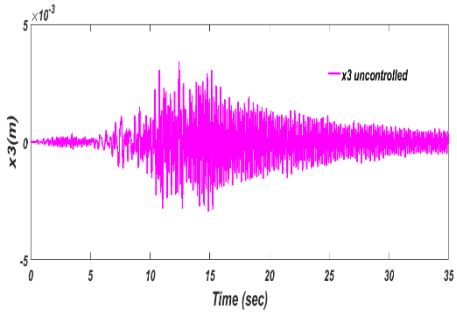

(c)

Figure 2. Uncontrolled system displacement under effect of Mexico City earthquake

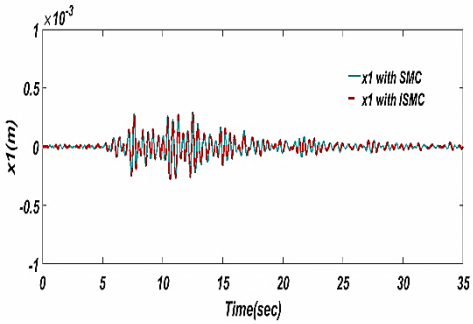

(a)

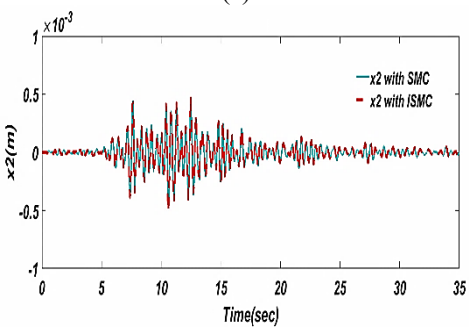

(b)

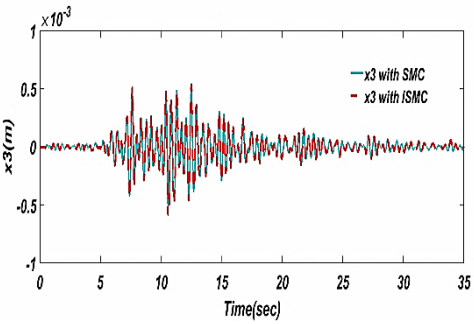

(c)

Figure 3. Displacement of three-story scaled structure controlled by SMS and ISMC

The controlled displacement with SMS and ISMC is shown in Figure 3.

The control force which is applied on the structure is shown in Figure 4.

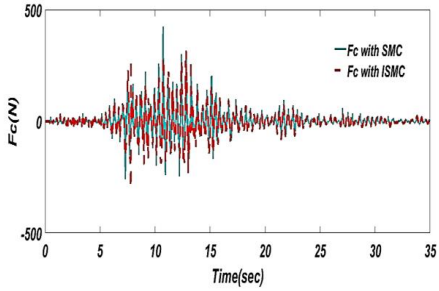

Figure 4. The control force with SMC and ISMC

The statistical results of the tow controllers results are given in Table 3.

Table 3. Maximum structural responses when structure is subjected to Mexico City earthquake

	Uncontrolled	SMC	ISMS
$x_1(m)$	0.002	0.0003	0.0003
$x_2(m)$	0.003	0.00048	0.00048
$x_3(m)$	0.0034	0.00058	0.00058
Control force(N)	/	425	314

From the previous result it is clear that the two controllers succeeded in reducing the structural displacement at the same rate, but ISMC can reduce the displacement with less control effort by about 33% compared to the maximum force by SMC as shown in Table 3.

Second scenario: To show the efficiency of ISMC control algorithm with the MRD, it will be compared to other controllers from the literature [23, 24] which used the same MRD and same structure which shown in Table 1 and Table 2 respectively under effect of Time scaled El Centro 1940 earthquake which shown in Figure 5.

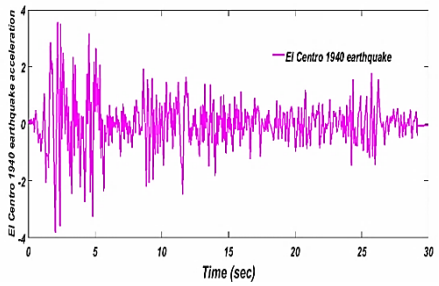

Figure 5. Time scaled El Centro 1940 earthquake acceleration

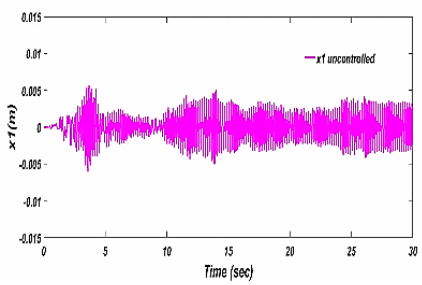

(a)

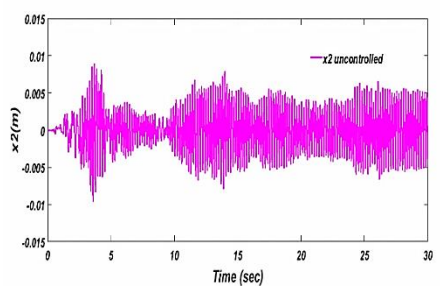

(b)

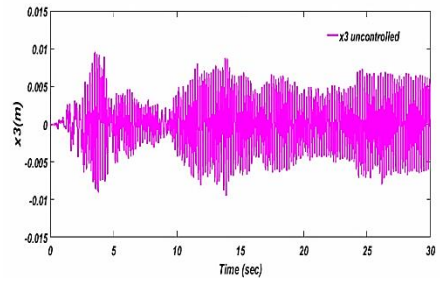

(c)

Figure 6. Uncontrolled displacement of three-story structure under effect of time scaled El Centro 1940 earthquake

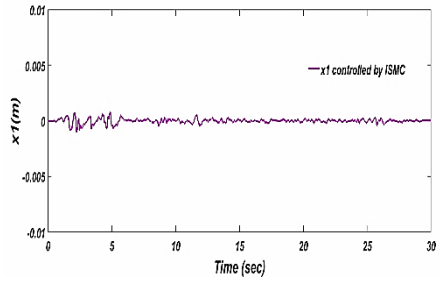

(a)

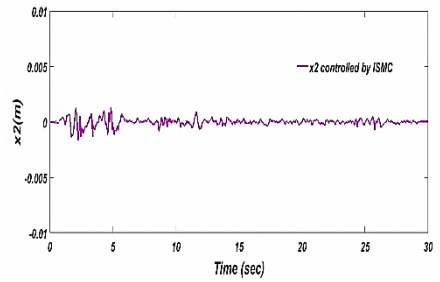

(b)

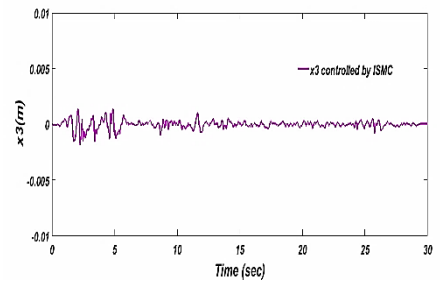

(c)

Figure 7. Displacement of three-story scaled structure under effect of El Centro 1940 earthquake controlled by ISMC

The uncontrolled displacement of three-story scaled structure under effect of time scaled El Centro 1940 earthquake are shown in Figure 6.

The displacement of three-story scaled structure under effect of time scaled El Centro 1940 earthquake controlled by ISMC shown in Figure 7.

The statistical results of the proposed controller under effect of El Centro 1940 earthquake are given in Table 4.

Table 4. Comparison of maximum structural responses between ISMC performance and the proposed controllers in [24, 25]

	Control strategy	x_3 *(m)*	F_c*(N)*
		0.0055	
1	Uncontrolled	0.0083	/
		0.0097	
		0.0021	
2	Passive off	0.0036	259.2
		0.0045	
		0.0008	
3	Passive on	0.002	992.8
		0.0031	
		0.0009	
4	Lyapunov controller (A)	0.0021	1023
		0.0031	
		0.0013	
5	Lyapunov controller (B)	0.0018	993.3
		0.0023	
		0.0013	
6	Quasi-bang-bang controller	0.0016	1002
		0.0023	
		0.0015	
7	Decentralized bang-bang controller	0.0025	923
		0.0032	
		0.0019	
8	Modulated homogenous friction controller	0.0029	503
		0.0038	
		0.0008	
9	Maximum energy dissipation controller	0.0020	993
		0.0031	
		0.0014	
10	Clipped-optimal controller	0.0021	918
		0.0026	
		0.0012	
11	Modified Quasi-bang-bang controller	0.0019	848.9
		0.0027	
		0.000787	
12	**ISMC**	**0.00126**	**682.2**
		0.00136	

From the comparison with the results that were obtained by [24, 25], notice that the proposed control technique is better in terms of control force than all control techniques except those proposed control algorithms No.2 and 8 respectively, but by observing the displacement which obtained by ISMC, ISMC result is better than the above two algorithms as well as from all control algorithms which proposed in [24, 25].

5. CONCLUSION

In this study ISMC is designed to drive MRD to reduce structure vibration for the first time. The main advantage which distinguishes ISMC from SMC is that ISMC does not have a reaching phase which means the system is in sliding from the first instant. ISMC can also attenuate the effect of unmatched disturbance by suitable choice of the sliding manifold. In addition, ISMC has better performance as compared to other control algorithms from the literature under the same simulation conditions.

As a future work, ISMC will be designed based on the barrier function to ensure a better robust behavior and simpler design requirement.

REFERENCES

[1] Han, S.W. (2020). Special issue on advanced methods for seismic performance evaluation of building structures. Applied Sciences, 10(20): 7353. https://doi.org/10.3390/app10207353

[2] Khatibinia, M., Mahmoudi, M., Eliasi, H. (2020). Optimal sliding mode control for seismic control of buildings equipped with ATMD. Iran University of Science & Technology, 10(1): 1-15. http://ijoce.iust.ac.ir/article-1-417-en.html.

[3] Ulusoy, S., Nigdeli, S.M., Bekdaş, G. (2021). Novel metaheuristic-based tuning of PID controllers for seismic structures and verification of robustness. Journal of Building Engineering, 33: 101647. https://doi.org/10.1016/j.jobe.2020.101647

[4] Yang, D.H., Shin, J.H., Lee, H., Kim, S.K., Kwak, M.K. (2017). Active vibration control of structure by active mass damper and multi-modal negative acceleration feedback control algorithm. Journal of Sound and Vibration, 392: 18-30. https://doi.org/10.1016/j.jsv.2016.12.036

[5] Xu, L., Cui, Y., Wang, Z. (2020). Active tuned mass damper based vibration control for seismic excited adjacent buildings under actuator saturation. Soil Dynamics and Earthquake Engineering, 135: 106181. https://doi.org/10.1016/j.soildyn.2020.106181

[6] Xu, L., Yu, Y., Cui, Y. (2018). Active vibration control for seismic excited building structures under actuator saturation, measurement stochastic noise and quantisation. Engineering Structures, 156: 1-11. https://doi.org/10.1016/j.engstruct.2017.11.021

[7] Kayabekir, A.E., Bekdaş, G., Nigdeli, S.M., Geem, Z.W. (2020). Optimum design of PID controlled active tuned mass damper via modified harmony search. Applied Sciences, 10(8): 2976. https://doi.org/10.3390/app10082976

[8] Husain, S.S., MohammadRidha, T. (2022). Integral sliding mode controlled ATMD for buildings under seismic effect. Under peer review process of International Journal of Safety and Security Engineering.

[9] Concha, A., Thenozhi, S., Betancourt, R.J., Gadi, S.K. (2021). A tuning algorithm for a sliding mode controller of buildings with ATMD. Mechanical Systems and Signal Processing, 154: 107539. https://doi.org/10.1016/j.ymssp.2020.107539

[10] Kavyashree, B.G., Patil, S., Rao, V.S. (2021). Review on vibration control in tall buildings: From the perspective of devices and applications. International Journal of Dynamics and Control, 9(3): 1316-1331. https://doi.org/10.1007/s40435-020-00728-6

[11] Owji, H.R., Shirazi, A.H.N., Sarvestani, H.H. (2011). A comparison between a new semi-active tuned mass damper and an active tuned mass damper. Procedia Engineering, 14: 2779-2787. https://doi.org/10.1016/j.proeng.2011.07.350

[12] Mahmoud, U.Y., Yasien, F.R., Ridha, T.M.M. (2009). Sliding Mode Control For Gust Responses In Tall Building. Engineering and Technology Journal, 27(5).

[13] Yu, W., Thenozhi, S. (2016). Active structural control with stable fuzzy PID techniques. Springer International Publishing.
[14] Yoon, D.S., Kim, G.W., Choi, S.B. (2021). Response time of magnetorheological dampers to current inputs in a semi-active suspension system: Modeling, control and sensitivity analysis. Mechanical Systems and Signal Processing, 146: 106999. https://doi.org/10.1016/j.ymssp.2020.106999
[15] Husain, S.S., MohammadRidha, T. (2022). Integral Sliding Mode Control for Seismic Effect Regulation on Buildings Using ATMD and MRD. Will be published in the fourth issuein Journal Européen des Systèmes Automatisé.
[16] Wang, J., Liu, Y., Qin, Z., Ma, L., Chu, F. (2022). Dynamic performance of a novel integral magnetorheological damper-rotor system. Mechanical Systems and Signal Processing, 172: 109004. https://doi.org/10.1016/j.ymssp.2022.109004
[17] Jagadisha, H.M., Rao, V.S. (2020). Classical PID controller for semi-active vibration control of seismically excited structure using magneto-rheological damper. In Global Challenges in Energy and Environment, pp. 201-210. https://doi.org/10.1007/978-981-13-9213-9_19
[18] Zizouni, K., Bousserhane, I.K., Hamouine, A., Fali, L. (2017). MR Damper-LQR control for earthquake vibration mitigation. International Journal of Civil Engineering and Technology (IJCIET), 8(11): 201-207.
[19] Zizouni, K., Fali, L., Sadek, Y., Bousserhane, I.K. (2019). Neural network control for earthquake structural vibration reduction using MRD. Frontiers of Structural and Civil Engineering, 13(5): 1171-1182. http://dx.doi.org/10.1007/s11709-019-0544-4
[20] Humaidi, A.J., Sadiq, M.E., Abdulkareem, A.I., Ibraheem, I.K., Azar, A.T. (2021). Adaptive backstepping sliding mode control design for vibration suppression of earth-quaked building supported by magneto-rheological damper. Journal of Low Frequency Noise, Vibration and Active Control, 41(2): 768-783. https://doi.org/10.1177/14613484211064
[21] Fali, L., Djermane, M., Zizouni, K., Sadek, Y. (2019). Adaptive sliding mode vibrations control for civil engineering earthquake excited structures. International Journal of Dynamics and Control, 7(3): 955-965. https://doi.org/10.1007/s40435-019-00559-0
[22] Hameed, A.H., Al-Dujaili, A.Q., Humaidi, A.J., Hussein, H.A. (2019). Design of terminal sliding position control for electronic throttle valve system: A performance comparative study. International Review of Automatic Control, 12(5): 251-260. https://doi.org/10.15866/ireaco.v12i5.16556
[23] Hamayun, M.T., Edwards, C., Alwi, H. (2016). Fault tolerant control schemes using integral sliding modes. Switzerland: Springer International Publishing.
[24] Joo, Y.H. (2022). Integral sliding mode control for increasing maximum power extraction efficiency of variable-speed wind energy system. International Journal of Electrical Power & Energy Systems, 139: 107958. https://doi.org/10.1016/j.ijepes.2022.107958
[25] Manzanilla, A., Ibarra, E., Salazar, S., Zamora, Á.E., Lozano, R., Munoz, F. (2021). Super-twisting integral sliding mode control for trajectory tracking of an Unmanned Underwater Vehicle. Ocean Engineering, 234: 109164. https://doi.org/10.1016/j.oceaneng.2021.109164
[26] Aly, A.M. (2013). Vibration control of buildings using magnetorheological damper: A new control algorithm. Journal of Engineering. https://doi.org/10.1155/2013/596078
[27] Dyke, S.J., Spencer, B.F. (1997). A comparison of semi-active control strategies for the MR damper. In Proceedings Intelligent Information Systems. IIS'97, pp. 580-584. https://doi.org/10.1109/IIS.1997.645424
[28] Ridha, T.M.M. (2010). The Design of a Tuned Mass Damper as a Vibration Absorber. Engineering and Technology Journal, 28(14).
[29] Rakan, A.B., MohammadRidha, T., AL-Samarraie, S. A. (2022). Artificial pancreas: Avoiding hyperglycemia and hypoglycemia for type one diabetes. International Journal on Advanced Science, Engineering and Information Technology, 12(1): 194-201. https://doi.org/10.18517/ijaseit.12.1.15106
[30] Humaidi, A.J., Hasan, S., Al-Jodah, A.A. (2018). Design of second order sliding mode for glucose regulation systems with disturbance. International Journal of Engineering & Technology, 7(2.28): 243-247. http://dx.doi.org/10.14419/ijet.v7i2.28.12936
[31] Ezzaldean, M.M., Kadhem, Q.S. (2019). Design of control system for 4-switch bldc motor based on sliding-mode and hysteresis controllers. Iraqi Journal of Computers, Communications, Control and Systems Engineering, 19(1): 42-51. https://doi.org/10.33103/uot.ijccce.19.1.6
[32] AL-Samarraie, S.A., Badri, A.S., Mishary, M.H. (2015). Integral sliding mode control design for electronic throttle valve system. Al-Khwarizmi Engineering Journal, 11(3): 72-84.
[33] De Loza, A.F., Bejarano, F.J., Fridman, L. (2013). Unmatched uncertainties compensation based on high-order sliding mode observation. International Journal of Robust and Nonlinear Control, 23(7): 754-764. https://doi.org/10.1002/rnc.2795
[34] Pan, Y., Yang, C., Pan, L., Yu, H. (2017). Integral sliding mode control: Performance, modification, and improvement. IEEE Transactions on Industrial Informatics, 14(7): 3087-3096. https://doi.org/10.1109/TII.2017.2761389
[35] Al-Dujaili, A.Q., Falah, A., Humaidi, A.J., Pereira, D.A., Ibraheem, I.K. (2020). Optimal super-twisting sliding mode control design of robot manipulator: Design and comparison study. International Journal of Advanced Robotic Systems, 17(6): 1729881420981524. https://doi.org/10.1177%2F1729881420981524

NOMENCLATURE

To show the efficiency of ISMC control algorithm with optimal design of sliding manifold, ISMC with classical and optimal design of sliding manifold are compared under effect of El Centro 1940 earthquake. The controlled displacement of three-story scaled structure which is parameter shown in Table 1, supported by MRD driven by ISMC are shown in Figure 8.

The statistical results of the ISMC with optimal and classical choice of sliding manifold under effect of El Centro 1940 earthquake are given in Table 5.

From the previous result show that performance of ISMC with optimal design of sliding manifold is relatively better than performance of ISMC with classical design of sliding manifold.

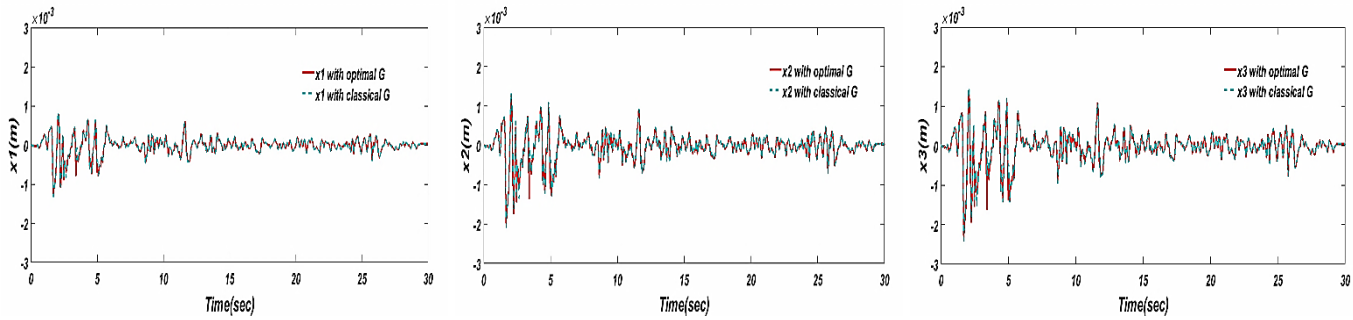

(a) (b) (c)

Figure 8. The control displacement by ISMC with optimal and classical design G

Table 5. Maximum structural responses with ISMC with classical and optimal design of sliding manifold

	Classical G	**Optimal G**
$x_1(m)$	0.00086	0.000787
$x_2(m)$	0.00136	0.00126
$x_3(m)$	0.00144	0.00136
Control force(N)	704.4	682.2